Oncogene (2005) 24, 3583–3595

www.nature.com/onc

Cell-autonomous induction of functional tumor suppressor 15-lipoxygenase 2 (15-LOX2) contributes to replicative senescence of human prostate progenitor cells

Bobby Bhatia[1], Shaohua Tang[1], Peiying Yang[2], Andreas Doll[3], Gerhard Aumüeller[3], Robert A Newman[2] and Dean G Tang*[,1]

[1]*Department of Carcinogenesis, The University of Texas MD Anderson Cancer Center, Science Park-Research Division, 1808 Park Rd. 1C, Smithville, TX 78957, USA;* [2]*Department of Experimental Therapeutics, The University of Texas MD Anderson Cancer Center, Houston, TX 77030, USA;* [3]*Department of Anatomy and Cell Biology, University of Marburg, Marburg, Germany*

Normal human prostatic (NHP) epithelial cells undergo senescence *in vitro* and *in vivo*, but little is known about the tissue-specific molecular mechanisms. Here we first characterize young primary NHP cells as CK5$^+$/CK18$^+$ intermediate basal cells that also express several other putative stem/progenitor cell markers including p63, CD44, $\alpha2\beta1$, and hTERT. When cultured in serum- and androgen-free medium, NHP cells gradually lose the expression of these markers, slow down in proliferation, and enter senescence. Several pieces of evidence implicate 15-lipoxygenase 2 (15-LOX2), a molecule with a restricted tissue expression and most abundantly expressed in adult human prostate, in the replicative senescence of NHP cells. *First*, the 15-LOX2 promoter activity and the mRNA and protein levels of 15-LOX2 and its multiple splice variants are upregulated in serially passaged NHP cells, which precede replicative senescence and occur in a cell-autonomous manner. *Second*, all immortalized prostate epithelial cells and prostate cancer cells do not express 15-LOX2. *Third*, PCa cells stably transfected with 15-LOX2 or 15-LOX2sv-b, a splice variant that does not possess arachidonate-metabolizing activity, show a passage-related senescence-like phenotype. *Fourth*, infection of early-passage NHP cells with retroviral vectors encoding 15-LOX2 or 15-LOX2sv-b induces partial cell-cycle arrest and big and flat senescence-like phenotype. *Finally*, 15-LOX2 protein expression in human prostate correlates with age. Together, these data suggest that 15-LOX2 may represent an endogenous prostate senescence gene and its tumor-suppressing functions might be associated with its ability to induce cell senescence.
Oncogene (2005) **24,** 3583–3595. doi:10.1038/sj.onc.1208406
Published online 7 March 2005

Keywords: 15-lipoxygenase 2; replicative cell senescence; stem cells; prostate progenitor cells; cell cycle; gene regulation

*Correspondence: DG Tang; E-mail: dtang@sprd1.mdacc.tmc.edu
Received 13 August 2004; revised 8 November 2004; accepted 26 November 2004; published online 7 March 2005

Introduction

Human prostatic glands consist of two major epithelial cell types: basal and secretory (lumenal). Basal cells express cytokeratin (CK) 5 and 14, whereas lumenal cells, which represent differentiated cells, express CK8 and 18, androgen receptor (AR), prostate-specific antigen (PSA) prostatic acid phosphatase (PAP), CD57 (Liu *et al*., 1997), and 15-LOX2 (Shappell *et al*., 1999; Tang *et al*., 2002). Evidence exists that in human prostate the basal cell compartment may contain putative stem and progenitor cells. *First*, ~80% of the proliferating cells are localized in the basal layer (Bonkhoff *et al*., 1994). *Second*, the majority of proliferating cells in the early outgrowth of the prostate explants are of the basal cell nature (Robinson *et al*., 1998; Hudson *et al*., 2000; Tran *et al*., 2002; Garraway *et al*., 2003). *Third*, some basal cells seem to have the ability to differentiate into lumenal cells (Robinson *et al*., 1998). *Finally*, several molecules known to play an important role in maintaining the stem/progenitor cell self-renewal and differentiation, including Notch-1 (Shou *et al*., 2001) and p63 (Signoretti *et al*., 2000), localize exclusively in the basal cell compartment in human prostate.

Recently, multiple adult human organs have been shown to contain stem cells (SC), that is, adult SC (Raff, 2003). Adult human prostate SC, which have not been definitively identified, are thought to localize in the basal cell compartment (Kinbara *et al*., 1996; Hudson *et al*., 2000) and appear to preferentially express cell surface molecules CD44 (Liu *et al*., 1997), $\alpha2\beta1$ (Collins *et al*., 2001), and CD133 (Richardson *et al*., 2004). The existence of SC in adult human prostate is supported by the ability of a small population of cells to form glandular-like structures in reconstituted systems (Hudson *et al*., 2000; Collins *et al*., 2001; Richardson *et al*., 2004). A small population of CK5 and CK18 double-positive (CK5$^+$/CK18$^+$) cells, called intermediate basal cells, has also been proposed to be prostate stem/progenitor cells (van Leenders *et al*., 2000; Schalken and van Leenders, 2003).

Adult human prostate is susceptible to two proliferative diseases: benign prostate hyperplasia (BPH), in which stromal cells are the major expanded cells, and prostate cancer (PCa), in which deregulated proliferation occurs mainly in the epithelial compartment. Among a multitude of environmental and genetic factors favoring PCa development, aging is the most significant risk factor: 15–30% of males >50 years and as many as 80% of the males >80 years harbor foci of PCa (Ruijter *et al*., 1999). How aging contributes to PCa development remains an enigma. Cultured NHP cells undergo replicative senescence after a period of proliferation and the process seems to involve the activation of both p16/pRb and p53/p21 pathways (Jarrard *et al*., 1999; Sandhu *et al*., 2000; Schwarze *et al*., 2001; Untergasser *et al*., 2002). Since replicative senescence is considered a barrier to immortalization and transformation (Hanahan and Weinberg, 2000; Wright and Shay, 2001; Schmitt *et al*., 2002), it is not surprising that multiple molecules (e.g., Rb, p53, and p16) involved in regulating cell senescence have been implicated in PCa development. SA-βgal-positive, senescent NHP cells have been detected in enlarged BPH prostates (Choi *et al*., 2000; Castro *et al*., 2003), but the roles of these cells in the etiology of BPH or PCa remain unclear.

Although molecules commonly involved in regulating replicative cell senescence have been implicated in NHP cell senescence, prostate-specific molecules that may play a specific role in NHP cell senescence have not been reported. Here we present evidence that 15-LOX2, which is most abundantly expressed in adult human prostate, is involved in NHP cell senescence.

Results

Characterization of NHP cells as CK5$^+$/CK18$^+$ intermediate basal cells that also express several other stem/progenitor cell markers

We first characterized primary NHP cells derived from multiple donors including NHP2 from a 59-year-old donor, NHP4 from a 17-year-old donor, NHP6 from a 28-year-old donor, and NHP7 from a 14-year-old donor. We generally obtained these cells at passage 2 (P2). Immunofluorescent staining revealed that all these NHP cells at P2 were CK5$^+$/CK18$^+$ and also expressed several other putative stem/progenitor cell markers including p63, hTERT, $\alpha2\beta1$, and CD44 (not shown). None of the NHP cells at P2 expressed lumenal markers 15-LOX2, AR, PSA, PAP, or CD57 (not shown).

NHP cells lose the progenitor cell markers in culture

Next, we followed changes in NHP cells, which had been constantly cultured and subcultured in serum- and androgen-free medium containing one survival factor (i.e., insulin) and one mitogen (i.e., EGF). NHP7 cells at P2 had undergone 19 population doublings (PDs) and 37% of the cells were proliferating upon a 4 h-BrdU pulse (Figure 1A, top). All cells were CK5$^+$/CK18$^+$ (Figure 1Aa–c) and positive for $\alpha2\beta1$ (Figure 1Ba), CD44 (Figure 1Be), and p63 (Figure 1Bi). At P3, NHP7 cells had undergone 22 PDs and proliferating cells dropped to 13% (Figure 1A). Accompanying the slowing down in cell proliferation were significantly increased cell sizes (Figures 1Ad–f and 2Bb, f). Most cells were still CK5$^+$/CK18$^+$ but some cells showed reduced CK18 expression (Figure 1Ad–f). Cell surface expression of $\alpha2\beta1$ (Figure 1Bb) and CD44 (Figure 1Bf) was observed in most cells, although more prominent cell–cell border staining was noticed for both molecules. Most cells still showed nuclear staining of p63 (Figure 1Bj).

By P4, NHP7 cells underwent only one extra PD and $\sim$9% of the cells incorporated BrdU (Figure 1A). One of the most prominent changes was the increased numbers of cells that had reduced or lost CK18 expression (Figure 1Ah), leading to significantly reduced numbers of CK5$^+$/CK18$^+$ cells (Figure 1Ai). The expression levels of $\alpha2\beta1$ (Figure 1Bc), CD44 (Figure 1Bg), and p63 (Figure 1Ak) were also significantly decreased in the majority of the cells. Some cells even completely lost the expression of these markers (e.g., Figure 1Bg, arrow). By P5, there was no further increase in PD and no cells incorporated BrdU (Figure 1A) upon a 4 h-pulse. All NHP7 cells at P5 had lost p63 expression (Figure 1Bl) and most ($\sim$95%) had lost $\alpha2\beta1$ (Figure 1Bd) and CD44 (Figure 1Bh) expression. Most cells also lost CK18 expression (e.g., Figure 1Aj–l) and the numbers of CK5$^+$/CK18$^+$ cells decreased to $\sim$5%.

To determine whether serially cultured NHP7 cells acquired any characteristics associated with differentiation, we stained cells of various passages for lumenal markers including CD57, PSA, AR, and PAP. We did not observe any positive cells for all four molecules (not shown). These observations together suggest that, as NHP7 cells gradually slow down in cell-cycle progression and approach their proliferative lifespan, they lose the expression of stem/progenitor cell markers without gaining differentiation markers. Similar results were also observed in serially passaged NHP6 cells (not shown).

Cell-autonomous upregulation of 15-LOX2 accompanies NHP cell senescence

The cell-cycle slowdown, loss of stem/progenitor properties, and prominent increases in cell sizes together suggest that the serially cultured NHP cells may be entering replicative senescence. We therefore examined this possibility, first, in NHP6 cells. NHP6 cells also showed an incremental decrease in their proliferative capacity as revealed by cumulative PDs and BrdU labeling (Figure 2A and C). As NHP6 cells declined in proliferation, many of the cells at P5 displayed enlarged and flattened morphology, contained prominent intracellular vacuoles, and stained positive for SA-βgal (Figure 2A and C), a marker of senescence (Dimri *et al*., 1995), suggesting that these cells were becoming senescent. By comparison, no NHP6 cells at $\leqslant$P4 were stained positive for SA-βgal (Figure 2A and C). At P6 and P7, SA-βgal$^+$ NHP6 cells increased to $\sim$50% and 90%, respectively (Figure 2A and C). On these

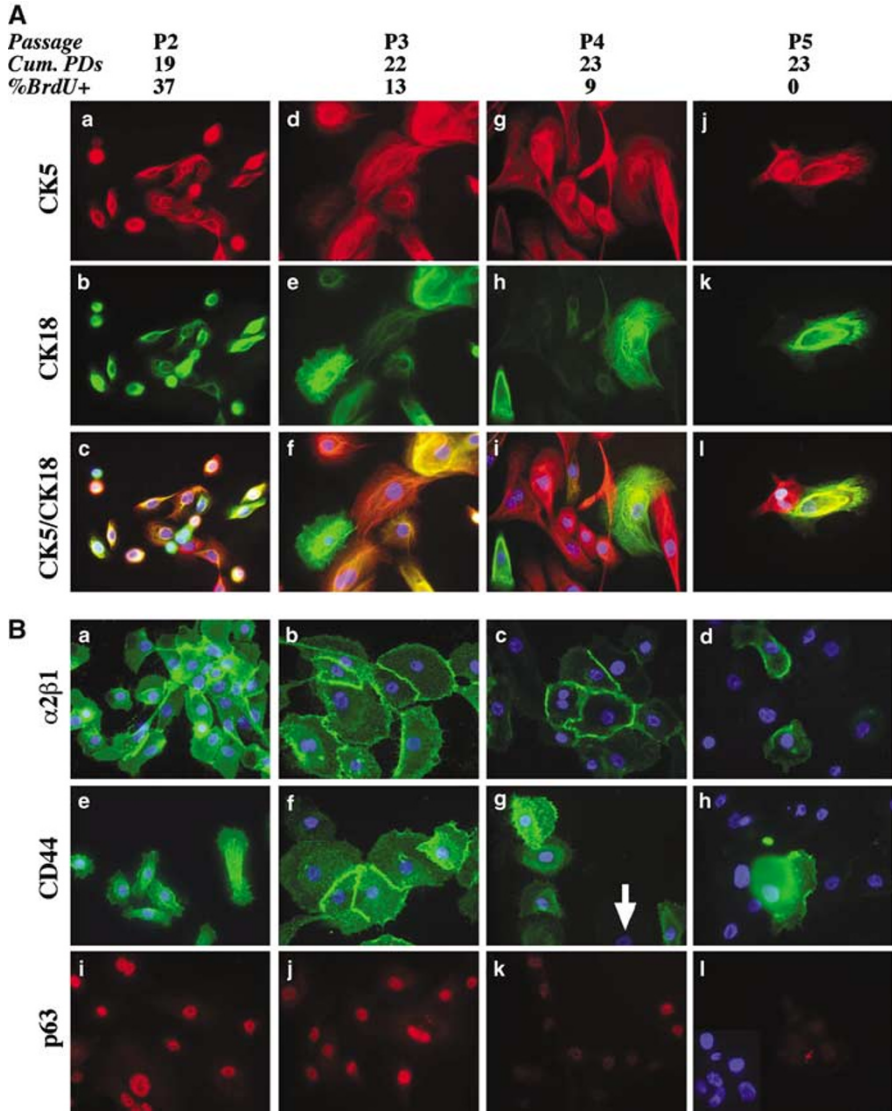

Figure 1 Cultured NHP cells gradually lose stem/progenitor cell properties. (**A**) NHP7 cells were double-stained for CK5 and CK18 and nuclei were counterstained by DAPI. The passage number, cumulative (cum.) PDs, and proliferating (i.e., $BrdU^+$) cells are indicated on top. (**B**) NHP6 cells were stained for $\alpha2\beta1$ (**a–d**), CD44 (**e–h**), or p63 (**i, j**). The arrow in (**g**) indicates a cell that has lost CD44 expression. The inset in (**l**) shows the nuclei of the cells stained for p63. Original magnifications: $\times 400$

observations, we designated the NHP6 cells at P2–P4 as young, P5–P6 as presenescent, and P7–P8 as senescent (Figure 2C).

Previously, we observed that primary NHP cells that expressed 15-LOX2, a molecule with a limited tissue distribution (i.e., prostate, lung, hair root, and cornea) and most abundantly expressed in adult prostate (Brash *et al*., 1997; Kilty *et al*., 1999), were generally big, flat, and cell-cycle arrested (Tang *et al*., 2002), raising the possibility that the 15-LOX2 may be associated with the NHP cell senescence. To test this possibility, we carried out triple staining for 15-LOX2, SA-βgal, and BrdU. The results indeed revealed a significantly increased 15-LOX2 expression in NHP6 cells as a function of cell-cycle arrest and replicative senescence (Figure 2A–C). At P2, no NHP6 cells stained positive for 15-LOX2 (not shown). At P3, $\sim$30% NHP6 cells were positive for 15-LOX2 (Figure 2A) and most of the 15-$LOX2^+$-NHP6 cells were BrdU-negative (Figure 2Cc). In contrast, $\sim$35% of the P3 15-LOX2-negative NHP6 cells were BrdU-positive (Figure 2Cc; Tang *et al*., 2002). By P5, $\sim$70% NHP6 cells became 15-$LOX2^+$ and $\sim$30% of the cells were SA-βgal^+ (Figure 2A and C). A 4-h BrdU pulse no longer labeled any proliferating cells (Figure 2Cf). By P7, nearly all NHP6 cells became strongly 15-$LOX2^+$ and $\sim$90% NHP6 cells stained positive for SA-βgal^+ (Figure 2A and C). There was a good correlation between SA-βgal staining and 15-LOX2 expression, that is, cells that were strongly 15-$LOX2^+$ were also strongly SA-βgal^+ (Figure 2Ce, f and Ch, i). The increased 15-LOX2 expression in cultured NHP6 cells was verified by Western blotting (see Figure 4A). Interestingly, at all passages analysed, the percentage of 15-$LOX2^+$ cells was higher than that of the SA-βgal^+ cells (Figure 2A)

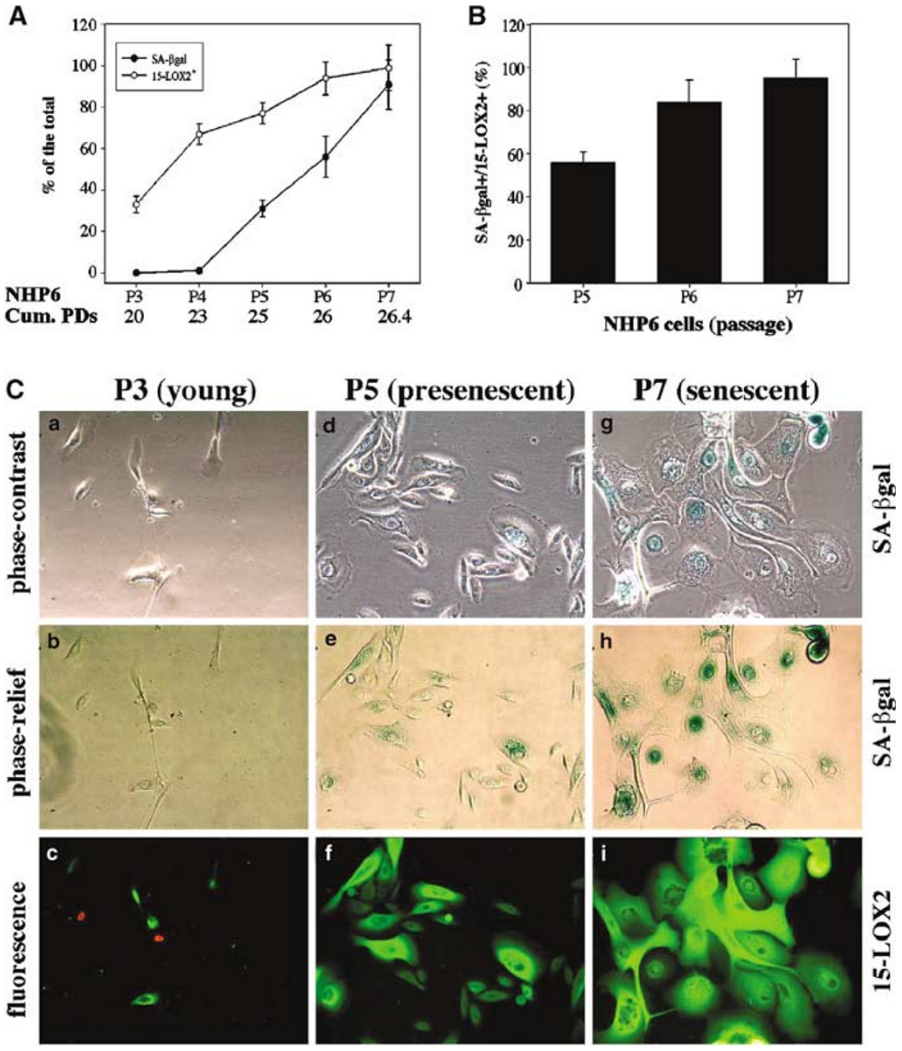

Figure 2 Induction of 15-LOX2 expression in NHP6 cells accompanies replicative cell senescence. (**A**) Quantifications of SA-βgal+ and 15-LOX2+ cells. Triplicate flasks were used in staining and an average of 600–1200 cells was scored for each passage. The bars represent the mean$\pm$s.e.m. derived from two separate experiments. Indicated at the bottom are passage numbers and the corresponding PDs. (**B**) Quantification of SA-βgal and 15-LOX2 double-positive cells in NHP6 cultures. (**C**) Representative microphotographs showing NHP6 cells at P3, P5, and P7 stained for SA-βgal (top and middle panels), BrdU (red), and 15-LOX2 (green). The images in the middle panels were taken using the phase-relief contrast filters in order to clearly show the SA-βgal staining. For BrdU staining, cells were pulsed for 4 h. Original magnifications, $\times 200$

and the 15-LOX2$^+$ cells were much bigger than the 15-LOX2$^-$ cells (Figure 2C). A differential counting of the % of SA-βgal$^+$ cells in the 15-LOX2$^+$ population revealed that $\sim$55 and 90% of the 15-LOX2$^+$-cells were positive for SA-βgal at P3 and P7, respectively (Figure 2B). Of note, cell nuclei generally accumulated less 15-LOX2 such that many 15-LOX2$^+$ cells appeared to have a hole in the nuclear area (Figure 2Cc, f, i).

Similar 15-LOX2 upregulation was also observed in serially passaged NHP2 and NHP7 cells (Figure 3). NHP2 cells underwent $\sim$29 PDs by P5–P6 (Figure 3A) and 15-LOX2 expression in NHP2 cells was also inversely correlated with cell proliferation (Figure 3B). At P3, $\sim$35% of the NHP2 cells were actively incorporating BrdU (Figure 3B) and most of the BrdU$^+$ cells were negative for 15-LOX2 (Figure 3Dc). By contrast, $\sim$10% of the cells were 15-LOX2-positive (Figure 3B), most of which did not incorporate BrdU (Figure 3Dc). SA-βgal$^+$ cells were $<$2% (Figure 3Db). By P4–P5, 50–60% of NHP2 cells became 15-LOX2$^+$ and $\sim$20% of the cells were SA-βgal$^+$ (Figure 3B and Dd–f). A 4 h-BrdU pulse no longer labeled any cells (Figure 3Df). By P6, $\sim$100% of NHP2 cells became 15-LOX2$^+$ and 80% SA-βgal$^+$ (Figure 3Dg–i). Again there was a good correlation between SA-βgal staining intensity and 15-LOX2 level (Figures 3De, f and 4Dh, i) and 15-LOX2$^+$ cells were much bigger than 15-LOX2$^-$ cells (Figure 3Dc, f, i). Also, senescent NHP2 cells showed prominent intracellular vacuoles and appeared to accumulate less 15-LOX2 in the nuclei in some cells (Figure 3Di). As in NHP6 cells, a differential

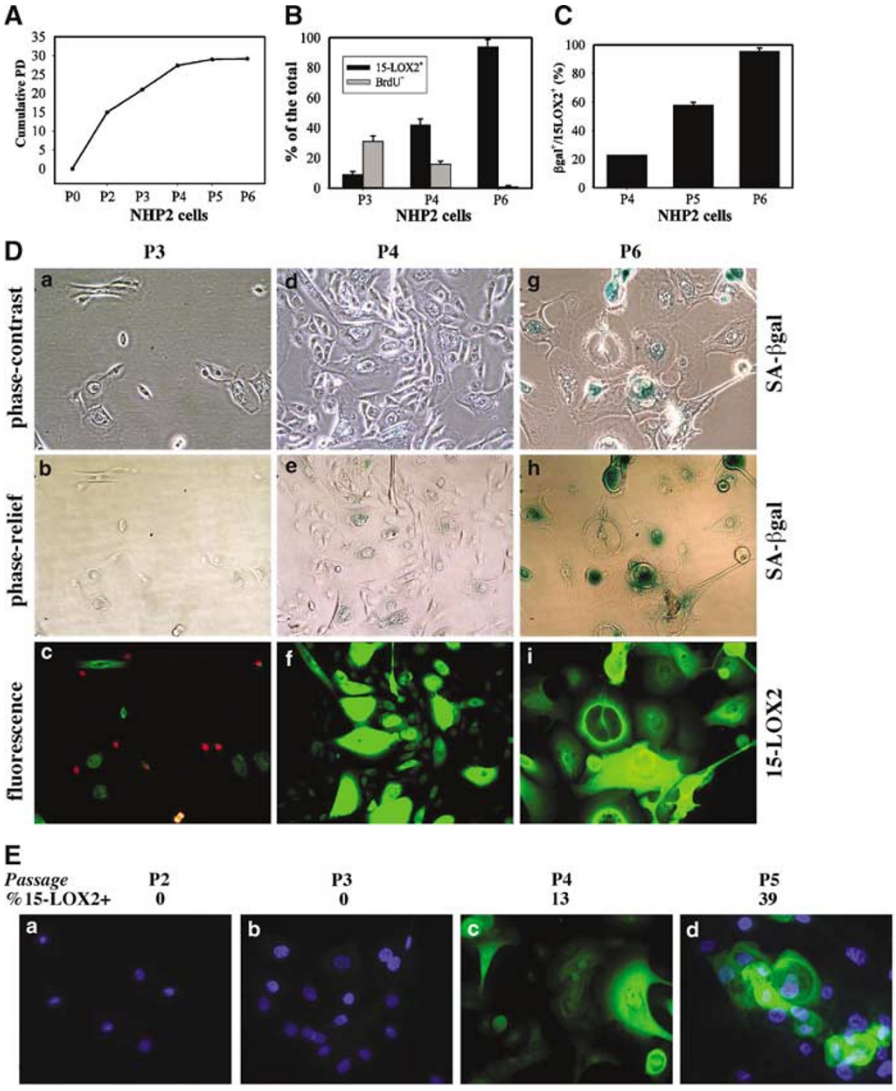

Figure 3 Induction of 15-LOX2 expression accompanies the replicative senescence of NHP2 (**A**–**D**) and NHP7 (**E**) cells. (**A**) Cumulative PDs. (**B**) NHP2 cells were processed for BrdU incorporation (4 h pulse) or 15-LOX2 staining. A total of 800–1200 cells was counted and the results are expressed as the mean ± s.e.m. from two experiments. (**C**) Quantification of SA-βgal and 15-LOX2 double-positive cells. (**D**) Representative microphotographs showing NHP2 cells stained for SA-βgal (top and middle panels), BrdU (4 h pulse; red), and 15-LOX2 (green). Original magnifications, $\times 200$. (**E**) Cell-autonomous induction of 15-LOX2 in NHP7 cells. The percentages of 15-LOX2$^+$ cells were determined by counting 500–800 cells at each passage. Original magnifications: $\times 400$

counting of the % of SA-βgal$^+$ cells in the 15-LOX2$^+$ population revealed that only a proportion of the 15-LOX2$^+$-NHP2 cells was SA-βgal$^+$ (Figure 3C).

Similar induction of 15-LOX2 was observed in NHP7 cells starting from P4 (Figure 3E). The percentages of SA-βgal$^+$ cells at P4–P7 were 0, 4, 40, and 75%, respectively, again suggesting that 15-LOX2 induction precedes senescence. Similar induction of 15-LOX2 was also observed in NHP4 cells (not shown).

Since all NHP cells had been constantly cultured in serum/androgen-free and semidefined conditions, these observations suggest that (1) 15-LOX2 is induced in NHP cells in a cell-autonomous manner, (2) 15-LOX2 induction occurs as NHP cells undergo replicative senescence, and (3) 15-LOX2 accumulation precedes cell senescence.

The upregulated 15-LOX2 in NHP cells is enzymatically active

15-LOX2 preferentially metabolizes arachidonic acid (AA) to generate a fatty acid, 15(S)-HETE (Brash *et al*., 1997; Kilty *et al*., 1999). To determine whether the upregulated 15-LOX2 in NHP cells is enzymatically active, we measured 15(S)-HETE levels in cultured NHP6 cells in the presence of AA. The results revealed increasing levels of 15(S)-HETE in NHP6 cells as a function of passage (Table 1), suggesting that the induced 15-LOX2 was enzymatically active. The P6 NHP6 cells produced >10 times more of 15(S)-HETE than the P3 NHP6 cells (Table 1). Surprisingly, when the measurement was done in the absence of AA, little 15(S)-HETE was detected in the P6 NHP6 cells

(Table 1). These results suggest that NHP cells normally cultured in the regular serum/androgen-free medium may produce little endogenous 15(S)-HETE. In support, measurement of the 15(S)-HETE levels in the culture media revealed barely detectable amounts (<0.02 ng/medium derived from 10^6 cells) in young (P2) and undetectable amounts in senescent (P7) NHP6 cells.

Transcriptional induction of both 15-LOX2 and its splice variants during NHP cell senescence

To determine whether 15-LOX2 induction resulted from transcriptional activation, we first measured the 15-LOX2 promoter activity in NHP6 cells transfected with the p15LOX2 ($-726/+80$)-luc reporter construct (Tang *et al*., 2004). As shown in Figure 4B, increasing 15-LOX2 promoter activity was observed in NHP6 cells with increasing passages. To confirm the promoter assays, we carried out semi-quantitative RT–PCR analysis. As shown in Figure 4C, 15-LOX2 mRNA levels increased as cells underwent senescence. RT–PCR using primers A and B, which detects 15-LOX2 and all its splice variants (Table 1S; Figure 1S; Tang *et al*., 2002), revealed that the total 15-LOX2 mRNA levels increased $\sim$2-fold from P3 to P4 and then further increased (by $\sim$5-fold) by P5–P6 (Figure 4C, top).

Previously, using long-distance RT–PCR, we identified three major 15-LOX2 splice variants named 15-LOX2sv-a, 15-OX2sv-b, and 15-LOX2sv-c (Figure 1S; Tang *et al*., 2002). During the present work, we identified two novel less abundant isoforms, which we named as 15-LOX2sv-d and 15-LOX2sv-e (Figure 4C and D; Figure 1S). 15-LOX2sv-d is identical to 15-LOX2, except that a 45-bp facultative intron in exon 9 (nt1302–nt1346) is spliced out. 15-LOX2sv-e is identical to 15-LOX2sv-c, except for the exon 9 being spliced out. To distinguish 15-LOX2 (i.e., full-length or FL) from its splicing isoforms, we carried out differential RT–PCR using several isoform-specific primers (Figure 4C–E; Table 1S; Figure 1S). The results demonstrated that 15-LOX2 and its splice variants (in particular, 15-LOX2sv-b) all increased, to different levels, in their mRNA levels during NHP cell senescence (Figure 4C–E). Interestingly, the upregulated mRNAs of 15-LOX2 and some of its variants slightly decreased in late-passage NHP6 cells (Figure 4C–E).

The RT–PCR results suggest that as NHP cells underwent senescence, the mRNA levels of both 15-

Table 1 15(S)-HETE production in NHP6 cells of different passages[a]

Passage	*15(S)-HETE level (ng/10^6 cells)*
Passage 3	1.25 ± 0.23
Passage 4	6.85 ± 0.05*
Passage 5	7.83 ± 0.28*
Passage 6	13.8 ± 2.4**
Passage 6[b]	0.27 ± 0.06

[a]15(S)-HETE production was measured in log-phase cells, in the presence of exogenous AA (100 μM; 37°C × 10 min) using LC/MS/MS. Data represent the mean$\pm$s.d. derived from 3–4 samples for each passage. *$P<0.01$ and **$P<0.001$, Student's *t*-test. [b]15(S)-HETE measurement in the absence of exogenous AA

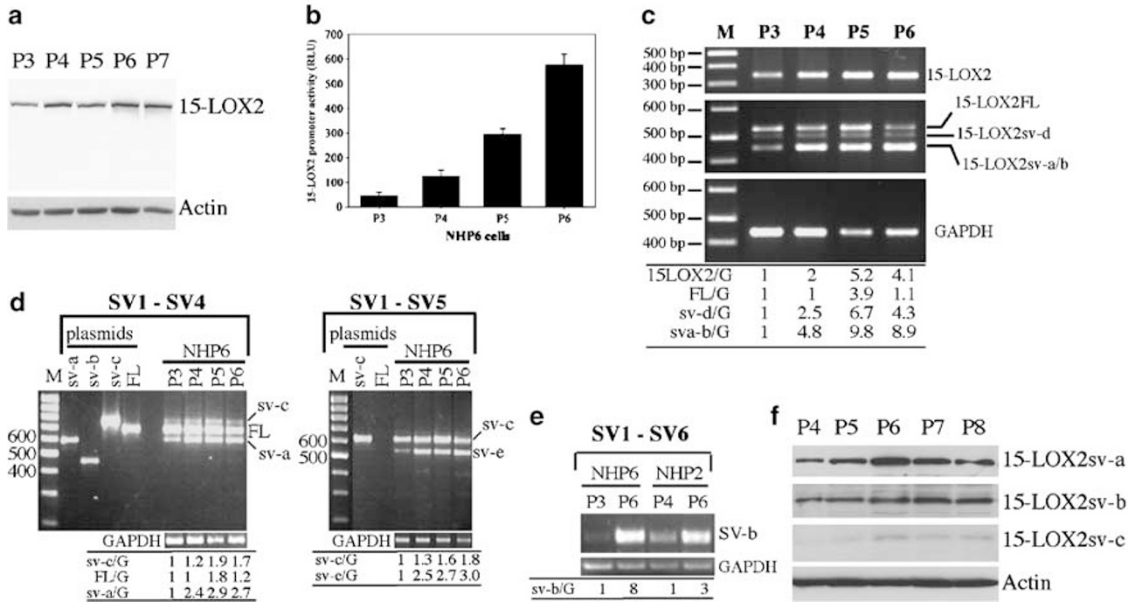

Figure 4 mRNA and protein induction of 15-LOX2 and its splice variants. (**a**) Western blotting (60 μg/lane) showing increased 15-LOX2 protein expression in passaged NHP6 cells. (**b**) Increased 15-LOX2 promoter activities in passaged NHP6 cells. The results were expressed as the relative luciferase unit (RLU) and the bars represent mean$\pm$s.e.m. from triplicate samples for each passage. (**c**–**e**) Increased mRNA levels of 15-LOX2 and its splice variants in NHP6 cells analysed by semiquantitative RT–PCR (see Table S1). The relative mRNA levels of 15-LOX2 or its variants over the corresponding GAPDH (**G**) mRNAs were determined by densitometric scanning. (**f**) 15-LOX2 splice variants were upregulated during NHP cell senescence. In all, 60 μg of NHP6 cell lysate was used in Western blotting using the newly generated peptide antibodies against individual 15-LOX2 isoforms

LOX2 and its splice variants were induced, leading to an increase in 15-LOX2 protein(s) detected on immunofluorescence. On Western blotting, the same rabbit polyclonal anti-15-LOX2 antibody also detected increased 15-LOX2 protein (Figure 4A). However, for unknown reasons, this antibody did not recognize the 15-LOX2 splice variants well on Western blotting (Figure 4A), as previously observed (Tang *et al*., 2002; Bhatia *et al*., 2003). To circumvent this problem, we made isoform-specific peptide polyclonal antibodies. Using these antibodies, we examined the protein levels of three major 15-LOX2 splice variants in passaged NHP6 cells. As shown in Figure 4F, 15-LOX2sv-a increased at P5, reached the peak level at P6, and then slightly decreased at P7-P8. By contrast, 15-LOX2sv-b continued to increase as a function of cell passage (Figure 4F). 15-LOX2sv-c showed similar changes as 15-LOX2sv-b although its expression levels were lower than those of 15-LOX2sv-b (Figure 4F).

Stable expression of 15-LOX2 or 15-LOX2sv-b in PC3 PCa cells results in a passage-related, senescence-like phenotype

In the following experiments, we attempt to determine whether 15-LOX2 induction causally contributes to NHP cell senescence. We first examined by Western blotting 15-LOX2 expression in both newly established and long-term cultured PCa cell lines (>15) as well as in several pairs of prostate epithelial cells immortalized by either viral oncogenes (i.e., SV40 large T antigen, HPV18, or E6/E7) or the catalytic subunit of human telomerase (hTERT) and their preimmortalized counterparts. We did not detect 15-LOX2 expression in any of the immortalized prostate epithelial or PCa cells (not shown), consistent with some of our earlier results (Tang *et al*., 2002). These observations suggest that 15-LOX2 expression is inversely correlated with cell immortality.

Next, we followed PC3 cells that had been stably transfected with 15-LOX2 or 15-LOX2sv-b (Bhatia *et al*., 2003) for multiple passages. These cells were derived from clonal cultures and enough cells generally became available for analysis only at P4–P5. To our surprise, these cells also showed passage-related phenotypic changes resembling replicative senescence in NHP cells. For instance, most of the early-passage (i.e., P3–P4) cells were generally small, actively proliferating, and SA-βgal-negative (not shown). By P6, 10–15% of the stably transfected cells became big and flat, some of which were also SA-βgal$^+$ (Figure 5a and b) and most of which were BrdU$^-$ (not shown). With increasing passage, the percentage of big/flat cells also increased in both 15-LOX2- and 15-LOX2sv-b-expressing PC3 cells (Figure 5a and b).

Enforced expression of 15-LOX2 or 15-LOX2sv-b in young NHP7 cells by retroviral infection also induces cell-cycle arrest and a senescence-like phenotype

Next, we carried out gain-of-function experiments in young NHP cells by taking advantage of the fact that NHP7 cells at P2 and P3 do not express 15-LOX2 and $\sim$14% of the cells start expressing 15-LOX2 at P4 (Figure 3E). Using two pBabe15LOX2-EGFP and two pBabe15LOX2sv-b-EGFP vectors and the pBabe-EGFP as control, we infected P2 NHP7 cells cultured at clonal density (i.e., 1000 cells/T25 slide flask). Triplicate slide flasks were terminated 1 week after infection and analysed for 15-LOX2 expression, BrdU incorporation, SA-βgal positivity, and morphological changes. As shown in Table 2 and Figure 6a, 82–96% of the P2 NHP7 cells were infected with the GFP-tagged retroviral vectors and the majority of the infected GFP$^+$ cells were positive for 15-LOX2. No 15-LOX2$^+$ cells were observed in uninfected or pBabe-EGFP-infected flasks (Table 2; Figure 6a). Some (8–22%) GFP$^+$ cells did not express 15-LOX2 (Table 2), perhaps because the retroviral LTR promoter was silenced. Interestingly, a very small percentage of (1–3%; Table 2) GFP$^-$ cells were 15-LOX2$^+$, possibly due to the inactivation of the pCMV promoter in these cells.

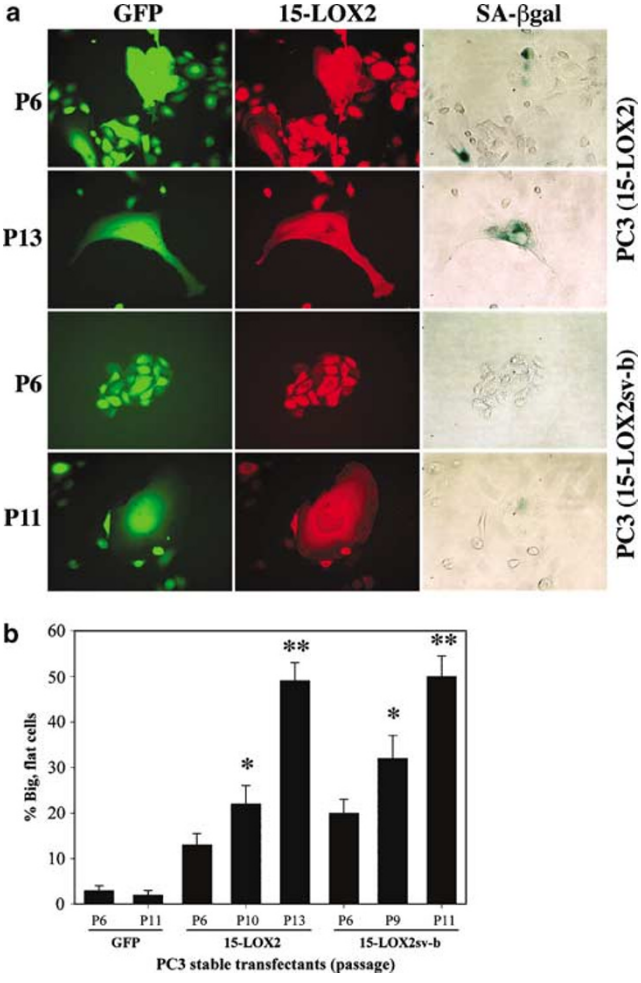

Figure 5 Stable overexpression of 15-LOX2 in PCa cells induces premature senescence. (**a**) PC3 cells stably transfected with 15-LOX2 or 15-LOX2sv-b at different passages were stained for 15-LOX2 (middle panels) and SA-βgal (right panels). (**b**) Quantification of senescence-like (big and flat) cells. $^*P<0.05$; $^{**}P<0.01$ (Student's *t*-test)

Table 2 15-LOX2 expression in NHP7 (P2) cells infected with retroviral expression vectors[a]

Cells	GFP+		*GFP*−	
	15-LOX2+	*15-LOX2*−	*15-LOX2*+	*15-LOX2*−
Uninfected	0	0	0	100%
pBabe-EGFP	0	67%	0	33%
pBabel5LOX2-EGFP (clone 3)	75%	8%	1%	16%
pBabel5LOX2-EGFP (clone 4)	73%	9%	3%	15%
pBabel5LOX2sv-b-EGFP (clone 1)	81%	11%	1%	8%
pBabel5LOX2sv-b-EGFP (clone 2)	74%	22%	0	4%

[a]NHP7 (P2) cells were plated in triplicate at clonal density (1000 cells/T25 slide flask) and either uninfected or infected with the indicated retroviral vectors. After 1 week, cells were fixed and processed for 15-LOX2 immunostaining. On average 200–300 cells were counted for each condition

When GFP$^+$/15-LOX2$^+$ and GFP$^+$/15-LOX2$^-$ NHP7 cells at P2 were compared at 7 days post infection for their morphology, many more of the GFP$^+$/15-LOX2$^+$ cells were big and flat (Figure 6a). Quantitative analyses revealed that both clones, each of 15-LOX2 and 15-LOX2sv-b retroviral vectors, increased the percentage of big and flat cells (Figure 6d). Infection with GFP-encoding retroviral vector also slightly increased the percentage of big and flat cells although the differences were not statistically significant (Figure 6d). As observed in stably transfected PC3 cells (Figure 6), only some of these big and flat cells stained strongly for SA-βgal (not shown). When GFP$^+$ and GFP$^-$ NHP7 cells at P2 were compared, at 7 days post infection, for BrdU incorporation, significantly more GFP$^-$ cells were found to be BrdU$^+$ (Figure 6b and c). Since the majority of GFP$^+$ cells were 15-LOX2$^+$ (Table 2), these results suggest that enforced 15-LOX2 expression in young NHP7 cells inhibits cell proliferation. Enforced expression of 15-LOX2sv-b similarly decreased BrdU$^+$ cells (Figure 6c) and increased the percentage of big and flat cells (Figure 6a and d).

Next, we asked how enforced 15-LOX2 expression might affect the long-term proliferation of young NHP7 cells. We similarly infected the clonally cultured P2 NHP7 cells with various retroviral vectors and followed these cells for 5 weeks. As shown in Figure 7, by 5 weeks, the initially plated 1000 cells either uninfected (a–e) or infected with pBabe-EGFP (f–j) proliferated extensively resulting in nearly confluent cultures. Little or only faint 15-LOX2 expression was detected in these cells (Figure 7c and h). By contrast, NHP7 cells infected with pBabe15-LOX2 only marginally increased in cell number and most of the infected cells were 15-LOX2$^+$ with enlarged and flattened morphology (Figure 7k–o). Surprisingly, NHP7 cells infected with pBabe15-LOX2sv-b, which initially behaved like the cells infected with the pBabe15LOX2-EGFP, gradually picked up proliferation and eventually resulted in confluent cultures (Figure 7p–t). Most of these cells were GFP$^+$ although a significant percentage of the cells was GFP$^-$ (Figure 7t). 15-LOX2 staining revealed that the majority of these cells had lost 15-LOX2 expression (Figure 7r) and only a few of the 15-LOX2$^+$, big and flat cells could be observed (not shown). Several replicate experiments with triplicate flasks infected with two clones each of 15-LOX2 or 15-LOX2sv-b revealed similar results (Figure 7 and data not shown).

15-LOX2 expression in human prostate appears to correlate with age

To determine whether 15-LOX2 expression *in vivo* might be associated with age, we carried out a pilot immunohistochemical survey of 15-LOX2 staining in human prostate tissues of various ages. As a control, these samples were also stained for PSA, an androgen-regulated gene. Both 15-LOX2 and PSA were negative in infant prostate tissues (not shown; $n=2$). In three samples of 15-year-old prostate, 15-LOX2 staining (Figure S2A) was negative although PSA staining was clearly positive (Figure S2B). 15-LOX2 staining became focally positive at age 18 (Figure S2C) and then significantly increased in adult prostates (Figure S2E; $n=3$). In the prostates of $\geqslant 50$ years ($n=2$), 15-LOX2 staining became homogeneously strong (Figure S2G). In the lumens of adult prostatic glands, 15-LOX2-positive secretions were easily observed (Figure S2E and G, arrows). In contrast, the PSA showed overall similar staining patterns and intensities in the $\geqslant 18$-year-old prostates (Figure S2D, F and H).

Discussion

The main goal of the present study was to study molecular mechanisms associated with the senescence of NHP cells. Our immunophenotyping experiments reveal that all young primary NHP cells are CK5$^+$/CK18$^+$ intermediate basal cells that also express p63, hTERT, CD44, and $\alpha 2\beta 1$, molecules proposed to mark prostate stem/progenitor cells (Liu *et al*., 1997; Signoretti *et al*., 2000; Collins *et al*., 2001). When serially cultured in the semidefined medium containing EGF and insulin, NHP cells gradually lose their proliferative potential and progenitor markers, suggesting that the simple culture conditions used here are insufficient to maintain the progenitor cell properties of the NHP cells. Interestingly, in a similar chemically defined medium containing PDGF and insulin, most perinatal rat oligodendrocyte precursor cells seem to be able to proliferate for years without losing progenitor markers (Tang *et al*., 2000,

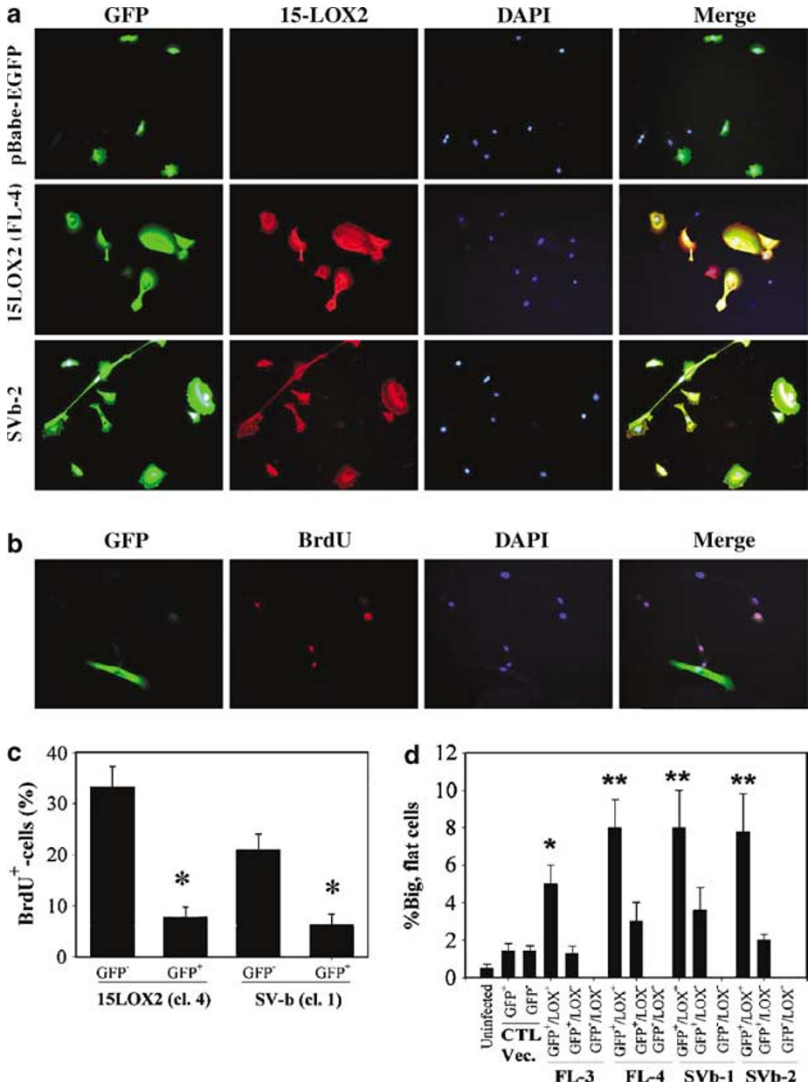

Figure 6 Enforced expression of 15-LOX2 or 15-LOX2sv-b in early-passage NHP7 cells induces cell-cycle arrest and a senescence-like phenotype. NHP7 cells at P2 were plated at clonal density were either untransduced or infected with pBabe-EGFP, pBabe15LOX2-EGFP (two clones used, that is, FL-3 and FL-4; see Table 2), or pBabe15LOXsv-b-EGFP (two clones used, that is, SVb-1 and SVb-2; see Table 2). After 1 week, cells were processed for 15-LOX2 (**a**), BrdU (**b**), or SA-βgal (not shown) staining. Representative images from one clone each of 15-LOX2 or 15-LOX2sv-b-infected cultures were shown. Original magnifications: $\times 200$. (**c**) The % of BrdU$^+$ cells was determined in the GFP$^+$ or GFP$^-$ population. The results represent the mean$\pm$s.d. $^*P<0.01$. (**d**) % (mean$\pm$s.d.) of big and flat cells. $^*P<0.01$; $^{**}P<0.001$

2001). It is unclear at the moment whether the different behaviors of these two cell types are caused by differences in cell lineages, initiating cell ages, or species.

Cultured NHP cells generally undergo a total of 23–30 PDs and their proliferative lifespan does not seem to be correlated with donor ages. For example, NHP7 cells derived from a 14-year-old donor undergo $\sim$23 PDs, whereas NHP2 cells derived from a 59-year-old donor undergo $\sim$30 PDs. This lack of correlation between donor age and cumulative PDs of NHP cells resembles that in human fibroblasts (Cristofalo *et al*., 1998). NHP cells undergo replicative senescence evidenced by cessation of proliferation, loss of progenitor properties, enlarged and flattened morphology, and expression of SA-βgal. Both presenescent and fully senescent NHP cells in culture do not acquire any differentiation markers such as AR, PSA, and PAP, molecules expressed mainly in the lumenal cells. Strikingly, 15-LOX2, another lumenal cell-specific molecule, is induced accompanying cell senescence under the non-differentiating culture conditions. Both 15-LOX2 and its splice variants are induced and the induction takes place in a cell-autonomous manner at the transcription level. How 15-LOX2 gene transcription is activated remains to be investigated although it does not seem to involve androgen/AR pathway as there is no androgen in the medium and NHP cells have always been AR-negative at the protein level. Moreover, androgen/AR pathway does not directly regulate the 15-LOX2 gene expression in NHP cells (Tang *et al*., 2004). One possibility is

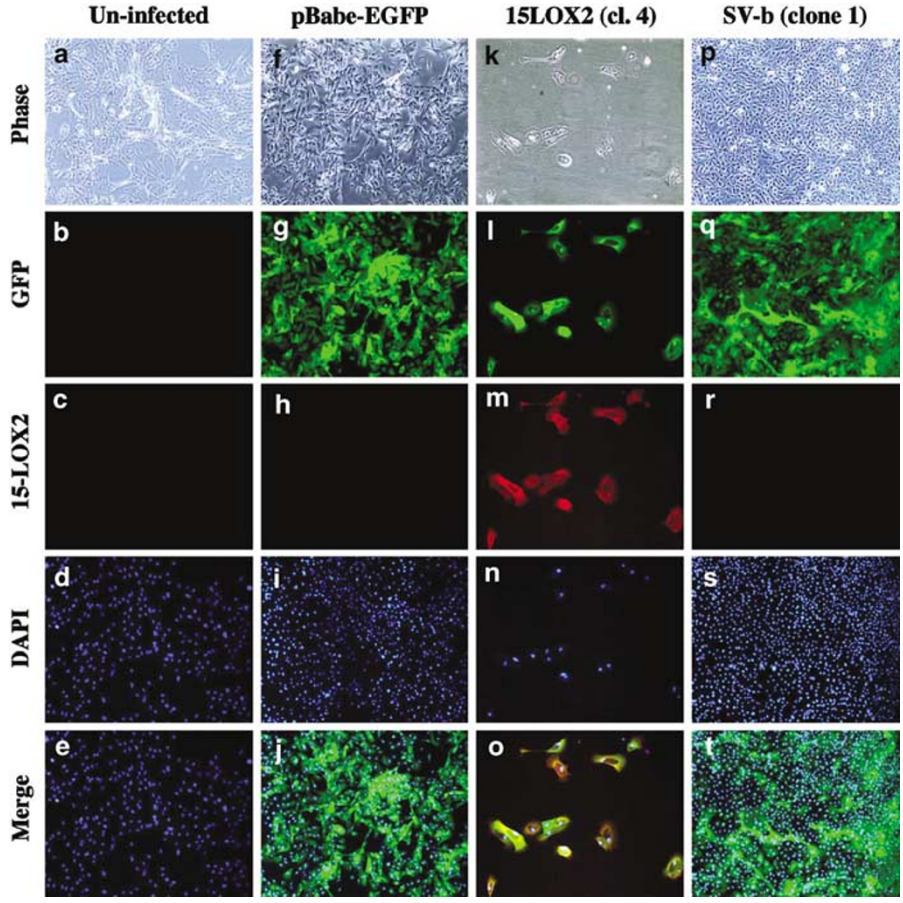

Figure 7 Enforced expression of 15-LOX2 inhibits long-term proliferation of NHP7 cells. NHP7 cells at P2 were infected as detailed in Figure 6 legend. Cells were processed for 15-LOX2 staining 5 weeks after infection. Representative images from one clone each of 15-LOX2 or 15-LOX2sv-b-infected cultures were shown. Original magnification: $\times 100$

through increased Sp1 transcriptional activity (Tang *et al*., 2004). In support, 15-LOX2 promoter constructs with the Sp1 sites mutated, when transfected into late-passage NHP6 cells, possess much lower promoter activities compared to the constructs with the intact Sp1 sites (Tang *et al*., 2004).

Several pieces of evidence suggest that induction and accumulation of 15-LOX2 and its splice variants may contribute to NHP cell-cycle arrest and senescence. *First*, 15-LOX2 expression is inversely correlated with NHP cell proliferation. *Second*, 15-LOX2 expression is inversely correlated with cell immortality. *Third*, 15-LOX2 behaves as a functional prostate tumor suppressor in that the 15-LOX2 mRNA, protein, and enzymatic activity are decreased or lost in PCa (Shappell *et al*., 1999) and re-expression of 15-LOX2 inhibits PCa cell proliferation *in vitro* and tumor development *in vivo* (Tang *et al*., 2002). *Fourth*, 15-LOX2 induction precedes the cell-cycle arrest and onset of NHP cell senescence. *Fifth*, remarkably, stable re-expression of 15-LOX2 in PCa cells, which apparently have bypassed the senescence checkpoint, also leads to a senescence-like phenotype. *Finally*, enforced expression of 15-LOX2 in young NHP cells results in a senescence-like phenotype. It is worth pointing out that enforced expression of 15-LOX2 in either young NHP or PCa cells does not seem to lead to a full manifestation of senescence as only a fraction of the cells is arrested in cell cycle and becomes big and flat and most of these big and flat, presumably senescent cells only stain weakly for SA-βgal. These results, which are not surprising, suggest that 15-LOX2 may represent only one of the multiple factors required to cause permanent cell-cycle exit and full senescence in NHP cells.

How does 15-LOX2 upregulation contribute to NHP cell senescence? As NHP cells undergo senescence, they upregulate cyclin-dependent kinase inhibitors (CKIs) p16 and p21. The downstream target of p16, pRb, as well as the upstream activator of p21, p53, are also upregulated (Bhatia *et al*., unpublished observations). Together, their concerted action may arrest NHP cells in the G1 phase of the cell cycle. How may 15-LOX2 expression contribute to CKI upregulation and cell cycle arrest? One possibility may be via its product, 15(S)-HETE, which has been proposed as a ligand PPAR-γ (Huang *et al*., 1999), the latter of which in turn may inhibit cell-cycle progression by inhibiting cyclin D1 (Wang *et al*., 2001). Although the 15-LOX2/15(S)-

HETE/PPARγ pathway cannot be excluded, several pieces of evidence suggest that the 15-LOX2-associated NHP cell senescence might not depend on AA metabolism and 15(S)-HETE production. *First*, although the induced 15-LOX2 is enzymatically active, late-passage/senescent NHP cells do not produce more endogenous 15(S)-HETE than the young NHP cells, nor do they secrete 15(S)-HETE into the medium. *Second*, although exogenous 15(S)-HETE can cause cell-cycle arrest in NHP or PCa cells, it does so only at high (i.e., μM) concentrations and without inducing a senescence-like phenotype (Tang *et al*., 2002 and unpublished observations). *Third*, not only 15-LOX2 but also its splice variants are induced during NHP cell senescence. Most 15-LOX2 splice variants either have much reduced (e.g., for 15-LOX2sv-a; Kilty *et al*., 1999) or completely lack (e.g., 15-LOX2sv-b and 15-LOX2sv-c; Bhatia *et al*., 2003), the AA-metabolizing activity and do not produce appreciable amounts of 15(S)-HETE. *Fourth*, just as 15-LOX2sv-b possesses tumor-inhibitory effects (Bhatia *et al*., 2003), enforced expression of 15-LOX2sv-b in young NHP or PCa cells also induces cell-cycle arrest and a senescence-like phenotype. Interestingly, most NHP cells infected with 15-LOX2sv-b retroviral vectors lose the transgene expression by 5 weeks, proliferate fast, and populate the culture dishes. The underlying mechanisms remain to be determined.

These discussions support a dual-action model in which 15-LOX2 and its splice variants possess both AA-dependent and AA metabolism-independent biological activities (Bhatia *et al*., 2003). Another mammalian LOX, 15-LOX1, is well known to bind biological membranes and catalyse their degradation independently of fatty acid metabolism (Kuhn and Borngraber, 1999). 15-LOX2 also shows significant membrane-binding capacities (Bhatia *et al*., 2003). Our preliminary data suggest that 15-LOX2 accumulation results in alterations in organelle membranes and increased oxidative stress, consistent with the prominent cytoplasmic vacuoles in senescent NHP cells. Oxidative stress in NHP cells may theoretically trigger telomere attrition and deprotection leading to cell-cycle checkpoint responses and subsequent senescence.

In summary, we have presented evidence that 15-LOX2 is involved in NHP cell senescence in culture. Although the *in vivo* biological relevance of this finding with regard to prostate aging remains to be determined, it is of interest that 15-LOX2 expression appears to increase with age, suggesting that 15-LOX2 might represent an endogenous prostate senescence gene. This possibility is consistent with 15-LOX2 being expressed only in a limited number of human tissues (i.e., prostate, lung, hair root, and cornea) and expressed most abundantly in prostate. Studies in multiple NHP cells suggest a direct correlation between the 15-LOX2 expression levels and the senescence phenotype, that is, cells that are strongly 15-LOX2-positive also show a fully senescent phenotype: big/flat morphology, lack of progenitor markers, and SA-βgal-positive. These observations in NHP cells, together with the 15-LOX2-induced senescence phenotype in PCa cells, suggests that 15-LOX2 expression, or the chronic damage induced by 15-LOX2, may have to accumulate to a certain threshold to help trigger cell senescence and that *in vivo* the relative low levels of 15-LOX2 in young prostate may play a differentiation-related function, whereas accumulated 15-LOX2 or 15-LOX2-induced cellular damages in older prostate may contribute to the senescence and aging phenotype. As the biological essence of replicative senescence is cell-cycle arrest and senescence has been considered a critical barrier to acquisition of immortality and tumorigenic transformation, the results presented herein provide novel mechanistic insight on (1) the normal developmental history of prostate stem/progenitor cells, (2) molecular mechanisms underlying NHP cell senescence, and (3) how 15-LOX2 may suppress tumor development and why its expression is shut down in PCa cells.

Materials and methods

Cells and reagents

NHP2, NHP4, and NHP6 cells (Tang *et al*., 2002, 2004) and NHP7 cells (Clonetics) were cultured on collagen-coated dishes in serum- and androgen-free, PrEBM medium supplemented with insulin, EGF, hydrocortisone, bovine pituitary extract, and cholera toxin, and used at passage 2–8. Luciferase reporter plasmids and anti-15-LOX2 antibody were previously described (Bhatia *et al*., 2003; Tang *et al*., 2004). Other antibodies used in this study include: polyclonal anti-CK5 (BabCO), monoclonal anti-CK18 (clone RGE53; BD PharMingen), monoclonal anti-p63 (clone 4A4), PSA and AR (Santa Cruz), 2 monoclonal anti-CD44 (clone G44-26 from BD PharMingen and DF1485 from Santa Cruz), polyclonal anti-hTERT (AbCAM), monoclonal anti-CD57 (clone NK-1) and $\alpha 2\beta 1$ (PharMingen), and monoclonal anti-PAP (clone PASE/4LJ; Dako). Secondary antibodies were acquired from Amersham. 15-HETE and 15-HETE-d_8 were from Cayman. AA and butylated hydroxytulene (BHT) were obtained from Sigma.

Immunofluorescence

Basic procedures were described (Tang *et al*., 2002; Bhatia *et al*., 2003). For cytoskeletal proteins (i.e., CK5 and CK18), cells were fixed and permeabilized in methanol/acetone (1 : 1; -20°C) for 10 min and then used in immunostaining. Cells were both analysed for fluorescence intensity and quantified for % positive cells. For the latter, 600–1200 cells were counted for each condition. Statistical analyses were performed using Student's *t*-test.

Semi-quantitative RT–PCR

Total RNA was isolated from NHP cells and used in RT–PCR as detailed in Table 1S.

Cumulative BrdU labeling and determination of PDs

Cumulative PDs were determined using a modified 3T3 protocol. For cumulative BrdU labeling (Tang *et al*., 2000, 2001), NHP cells were pulsed with 10 μM BrdU for 2–120 h, fixed in 4% paraformaldehyde, permeabilized in 70% ethanol (in PBS, -20°C) for 10 min, and then incubated with monoclonal anti-BrdU antibody followed by goat anti-mouse IgG-Rhodamine. Finally, cells were nuclear counterstained

with DAPI. A total of 1000–1200 cells were counted per coverslip to determine the proportion of $BrdU^+$ cells. The labeling index was plotted against the BrdU pulse time to obtain a cumulative labeling curve. PD was determined using the formula $2^x = N_f/N_i$, where x is the PD, N_f is the final cell number and N_i is the number of cell initially plated. The approximate PD time was determined using the formula $d = t/\log_2 N$, where d is the PD time, t is the time of cells in culture, and N is the total number of cells.

Western blotting

Whole cell lysates were used in Western blotting using ECL (Tang *et al*., 2002; Bhatia *et al*., 2003).

Senescence-associated β-galactosidase (SA-βgal) staining

NHP cells of different passages were stained for SA-βgal (Dimri *et al*., 1995; Tang *et al*., 2001). In some experiments, triple staining of 15-LOX2, BrdU, and SA-βgal was carried out.

15-HETE measurement in NHP cells or culture medium by liquid chromatography and tandem mass spectrometry (LC/MS/MS)

15(S)-HETE levels in NHP cells were measured as previously detailed (Tang *et al*., 2002). Eicosanoids in culture medium were measured using a solid-phase method and the detailed protocol is available upon request.

Preparation of 15-LOX2 isoform-specific peptide antibodies

Peptide sequences at the splicing junctures (Tang *et al*., 2002) were utilized as immunogens to produce isoform-specific antibodies. Specifically, peptides YRDDGMQIWGIPSSLE (for 15-LOX2sv-b), HHPPPKAWQHARAS (for 15-LOX2sv-c), and HPLFKSTGIGIEGF (for 15-LOX2sv-a) were chemically synthesized by coupling to an N-terminal cysteine, HPLC purified, and then utilized to immunize the New Zealand White rabbit by intradermal injection. The antibodies produced were affinity-purified using the commercial Kit (Pierce, Rockford, IL, USA). The purified antibodies, together with the preimmune sera were characterized using PCa cells transfected with the individual cDNAs (Bhatia *et al*., 2003).

Retroviral experiments

We made several bi-cistronic pBabe-EGFP retroviral vectors in which 15-LOX2 or 15-LOX2sv-b is driven by the viral LTR, whereas GFP is expressed from the CMV promoter. 15-LOX2 or 15-LOX2sv-b cDNA was released from pCMS-EGFP-15LOX2 or pCMS-EGFP-15LOX2sv-b vectors (Bhatia *et al*., 2003) and the cDNAs were ligated into pBabe-EGFP (Tang *et al*., 2001) retroviral vector. Two 15-LOX2 and two 15-LOX2sv-b retroviral vectors were transfected into the Ampho-Phoenix packaging cells using FuGENE 6. At 48 h post transfection, viral particles were collected from the culture medium by ultracentrifugation and used to infect NHP cells (Tang *et al*., 2001).

Immunohistochemical staining of 15-LOX2 and PSA

Paraffin-embedded sections of archival prostate tissues of different ages, including infant (one 2-month-old, one 1-year-old), adolescent (three 15-year-old and one 18-year-old), adult (one case each of 36-, 38-, and 43-year-old), and senior (three 50-year-old and two 62-year-old), were used in staining for 15-LOX2 and PSA. Tissue sections were incubated with 3% H_2O_2 to block endogenous peroxidase activity and in 10 mM citrate buffer (pH 6.0) for 10 min in a microwave oven for antigen retrieval. Slides were then incubated in 10% goat whole serum in PBS for 30 min to block nonspecific binding and then in anti-15-LOX2 antibody. Finally, slides were incubated with anti-rabbit HRP (30 min at room temperature) and then with the substrate DAB.

Acknowledgements
We thank D Chopra and J Rhim for providing cells. This work is supported, in part, by NIH grants CA90297 and AG023374, ACS Grant RSG MGO-105961, DOD grant DAMD17-03-1-0137, University of Texas MDACC PCRP and IRG funds, and NIEHS Center Grant P50 ES07784 (all to DGT). RAN was supported by NCI Cancer Center Support grant CA16672 and P01 CA106451.

References

Bhatia B, Maldonado CJ, Tang S, Chandra D, Klein RD, Chopra D, Shappell SB, Yang P, Newman RA and Tang DG. (2003). *J. Biol. Chem.*, **278,** 25091–25100.
Bonkhoff H, Stein U and Remberger K. (1994). *Prostate*, **24,** 42–46.
Brash AR, Boeglin WE and Chang MS. (1997). *Proc. Natl. Acad. Sci. USA*, **94,** 6148–6152.
Castro P, Giri D, Lamb D and Ittman M. (2003). *Prostate*, **55,** 30–38.
Choi J, Shendrik I, Peacocke M, Peehl D, Buttyan R, Ikeguchi EF, Katz AE and Benson MC. (2000). *Urology*, **56,** 160–166.
Collins AT, Habib FK, Maitland NJ and Neal DE. (2001). *J. Cell Sci.*, **114,** 3865–3872.
Cristofalo VJ, Allen RG, Pignolo RJ, Martin BG and Beck JC. (1998). *Proc. Natl. Acad. Sci. USA*, **95,** 10614–10619.
Dimri GP, Lee X, Basile G, Acosta M, Scott G, Roskelley C, Medrano EE, Linskens M, Rubelj I, Pereira-Smith O, Peacocke M and Campisi J. (1995). *Proc. Natl. Acad. Sci. USA*, **92,** 9363–9367.
Garraway LA, Lin D, Signoretti S, Waltregny D, Dilks J, Bhattacharya N and Loda M. (2003). *Prostate*, **55,** 206–218.
Hanahan D and Weinberg RA. (2000). *Cell*, **100,** 57–70.
Huang JT, Welch JS, Ricote M, Binder CJ, Wilson TM, Kelly C, Witztum JL, Funk CD, Conrad D and Glass CK. (1999). *Nature*, **400,** 378–382.
Hudson DL, O'Hare M, Watt FM and Masters JRW. (2000). *Lab. Invest.*, **80,** 1243–1250.
Jarrard DF, Sarkar S, Shi Y, Yeager TR, Magrane G, Kinoshita H, Nassif N, Meisner L, Newton MA, Waldman FM and Reznikoff CA. (1999). *Cancer Res.*, **59,** 2957–2964.
Kilty I, Alison L and Vickers PJ. (1999). *Eur. J. Biochem.*, **266,** 83–93.
Kinbara H, Cunha GR, Boutin E, Hayashi N and Kawamura J. (1996). *Prostate*, **29,** 107–116.
Kuhn H and Borngraber S. (1999). *Adv. Exp. Med. Biol.*, **447,** 5–28.
Liu AY, True, LD, LaTray, L, Nelson PS, Ellis WJ, Vessella, RL, Lange, PH, Hood L and van den Engn G. (1997). *Proc. Natl. Acad. Sci. USA*, **94,** 10705–10710.
Raff M. (2003). *Annu. Rev. Cell Dev. Biol.*, **19,** 1–22.
Richardson GD, Robson CN, Lang SH, Neal DE, Maitland NJ and Collins AT.. (2004). *J. Cell Sci.* (E-pub June 29).

Robinson EJ, Neal DE and Collins AT. (1998). *Prostate*, **37,** 149–160.
Ruijter E, van de Kaa C, Miller G, Ruiter D, Debruyne F and Schalken J. (1999). *Endocr. Rev.*, **20,** 22–45.
Sandhu C, Peehl DM and Singerland J. (2000). *Cancer Res.*, **60,** 2616–2622.
Schalken JA and van Leenders G. (2003). *Urology*, **62,** 11–20.
Schmitt CA, Fridman JS, Yang M, Lee S, Baranov E, Hoffman RM and Lowe SW. (2002). *Cell*, **109,** 335–346.
Schwarze SR, Shi Y, Fu VX, Watson PA and Jarrard DF. (2001). *Oncogene*, **20,** 8184–8192.
Shappell SB, Boeglin WE, Olson SJ, Kasper S and Brash AR. (1999). *Am. J. Pathol.*, **155,** 235–245.
Shou J, Ross S, Koeppen H, de Sauvage FJ and Gao W-Q. (2001). *Cancer Res.*, **61,** 7291–7297.
Signoretti S, Waltregny D, Dilks J, Isaac B, Lin, D, Garraway L, Yang A, Montironi R, McKeon F and Loda M. (2000). *Am. J. Pathol.*, **157,** 1769–1775.
Tang DG, Tokumoto YM and Raff MC. (2000). *J. Cell Biol.*, **148,** 971–984.
Tang DG, Tokumoto YM, Apperly JA, Lloyd AC and Raff MC. (2001). *Science*, **291,** 868–871.
Tang S, Bhatia B, Maldonado C, Yang P, Newman RA, Liu J, Chandra D, Traag J, Klein RD, Fischer SM, Chopra D, Shen J, Zhau H, Chung LW-K and Tang DG. (2002). *J. Biol. Chem.*, **277,** 16189–16201.
Tang S, Bhatia B, Zhou J-J, Maldonado CJ, Chandra D, Kim E, Fischer S, Butler AF, Friedman SL and Tang DG. (2004). *Oncogene*, **23,** 6942–6953.
Tran CP, Lin C, Yamashiro J and Reiter RE. (2002). *Mol. Cancer Res.*, **1,** 113–121.
Untergasser G, Koch, HB, Menssen A and Hermeking H. (2002). *Cancer Res.*, **62,** 6255–6262.
van Leenders G, Dijkman H, van de Kaa H, Ruiter D and Schalken J. (2000). *Lab. Invest.*, **80,** 1251–1258.
Wang C, Fu M, A'Mico M, Albanese C, Zhou JN, Brownlee M, Lisanti MP, Chatterjee VKK, Lazar MA and Pestell RG. (2001). *Mol. Cell. Biol.*, **21,** 3057–3070.
Wright WE and Shay JW. (2001). *Curr. Opin. Genet. Dev.*, **11,** 98–103.

Supplementary Information accompanies the paper on Oncogene website (http://www.nature.com/onc)